

Liquid phase deposition of supramolecular monolayers of zinc porphyrin molecules on graphite

This article has been downloaded from IOPscience. Please scroll down to see the full text article.

2003 J. Phys.: Condens. Matter 15 S3127

(<http://iopscience.iop.org/0953-8984/15/42/010>)

View [the table of contents for this issue](#), or go to the [journal homepage](#) for more

Download details:

IP Address: 171.66.16.125

The article was downloaded on 19/05/2010 at 15:21

Please note that [terms and conditions apply](#).

Liquid phase deposition of supramolecular monolayers of zinc porphyrin molecules on graphite

Q Guo¹, J Yin¹, F Yin¹, R E Palmer¹, N Bampos² and J K M Sanders²

¹ Nanoscale Physics Research Laboratory, School of Physics and Astronomy,
University of Birmingham, Birmingham B15 2TT, UK

² Cambridge Centre for Molecular Recognition, University Chemical Laboratory,
University of Cambridge, Lensfield Road, Cambridge CB2 1EW, UK

E-mail: q.guo@bham.ac.uk

Received 4 July 2003

Published 10 October 2003

Online at stacks.iop.org/JPhysCM/15/S3127

Abstract

Molecular monolayers of zinc porphyrins deposited from liquid sources on graphite substrates have been characterized using atomic force microscopy. The morphology of the molecular layers shows a strong dependence on both the structure of the individual molecules and the properties of the solvent used for the deposition. By controlling the concentration of the starting solution and the amount of liquid applied to the graphite surface, single layer high molecular weight films have been successfully grown with a variety of zinc porphyrin molecules. The nucleation and growth, similar to those commonly observed in vapour deposition, have been found to depend on the strength of the intermolecular interaction as well as the level of interaction between the solvent molecules and the substrate.

1. Introduction

The development of molecular electronic devices requires a thorough understanding of electron transport mechanisms across molecules or assemblies [1–8]. In comparison with the wealth of knowledge accumulated on electron transport processes in inorganic crystalline solids, much less is known about the fine details of these processes in molecular solids. This is partly due to the complexity of the structure of molecular solids, in which molecules are usually linked via relatively weak van der Waals forces, while long range order is also often poor or even non-existent. Another important issue related to molecular electronic devices is that an operational molecular device is usually built on top of a solid substrate which, in addition to providing a rigid support for the molecular structure, offers interconnection possibilities. In some cases, the substrate itself plays an important role in the functioning of the molecular device. Therefore, when designing any new molecular device, one needs to consider not

only the way the molecules interact with one another, but also the effect of the substrate on the ordering and orientation of the molecules. In this paper we address these two issues, using the adsorption of zinc porphyrin molecules (including supramolecular assemblies) on the conducting graphite surface as an example, and demonstrate how in practice the structure of molecular monolayers can be controlled by varying the structure of the individual molecules as well as by choosing different solvents.

Porphyrin molecules have a variety of important properties, such as their characteristic absorption spectra in the visible range [9–11]. Because of their interesting optical behaviour, porphyrin molecules and their corresponding supramolecular structures have been investigated as artificial light harvesting antennae [12]. The porphyrins are also electrically conductive, which is useful for device fabrication, and also allows the molecules to be imaged with the scanning tunnelling microscope [13–15]. Other molecules with similar electronic and optical properties to the porphyrins have also attracted much attention from the scientific community in recent years. For instance, the adsorption of PTCDA (perylene tetracarboxylic acid dianhydride) [16], TTF-TCNQ [17] and phthalocyanines [18] on a variety of substrates has been investigated.

Molecular layers supported on a solid substrate can be prepared by two routes: (a) vacuum sublimation/evaporation and (b) liquid phase deposition. The former has the advantage that the deposition process can be conducted and controlled with extremely high precision; e.g., in principle it is possible to deposit one molecule at a time (see [19] for a recent review and [20] for some recent reports of porphyrin adsorption on metal substrate prepared by sublimation). However, higher temperatures are usually required for the sublimation of structurally more complex molecules and this may lead to fragmentation of the molecules in the deposition process. Deposition from the liquid phase, as used successfully to deposit 'thick' (>10 nm) layers of polymeric photoresist in microfabrication processes, avoids the risk of molecular fragmentation and is also an economical process. Although in many cases the degree of control over the coverage and morphology of the molecular film is not as strong as in vacuum sublimation, accuracy at the molecular level has been achieved, for example, in the case of self-assembled monolayers of alkanethiols on the (111) surface of gold [21]. Recent work carried out in our laboratory [22] has demonstrated the controlled formation of porphyrin monolayers on graphite via liquid phase deposition.

2. Experimental details

2.1. The molecules

All the zinc porphyrin molecules (including the supermolecular assemblies) employed in our investigation were synthesized at Cambridge University [23]. Figure 1 shows the molecular structures of the four zinc porphyrin molecules discussed in this paper. Figures 1(a) and (b) show the structures of two monomeric zinc porphyrin isomers; both have two trimethylsilane (TMS) groups bonded to the macrocycle via phenyl groups and acetylene linkers, as well as four ester side chains. The only difference between the isomers is in the position of the two acetylene linkers on the phenyl rings. For isomer **I** the linkers are *meta*-substituted, while for isomer **II** they are *para*-substituted. For both isomers, the minimum energy configuration is the one with the phenyl rings perpendicular to the macrocycle. These two isomers were selected to study the effect of the molecular structure on the morphology of the molecular films. Figure 1(c) shows a zinc porphyrin trimer (ZPT) molecule. This molecule has a cavity in the middle and is composed of three butadiyne-linked diarylporphyrin monomers. There are four ester side chains substituted onto each porphyrin ring, giving a total of 12 side chains in the whole

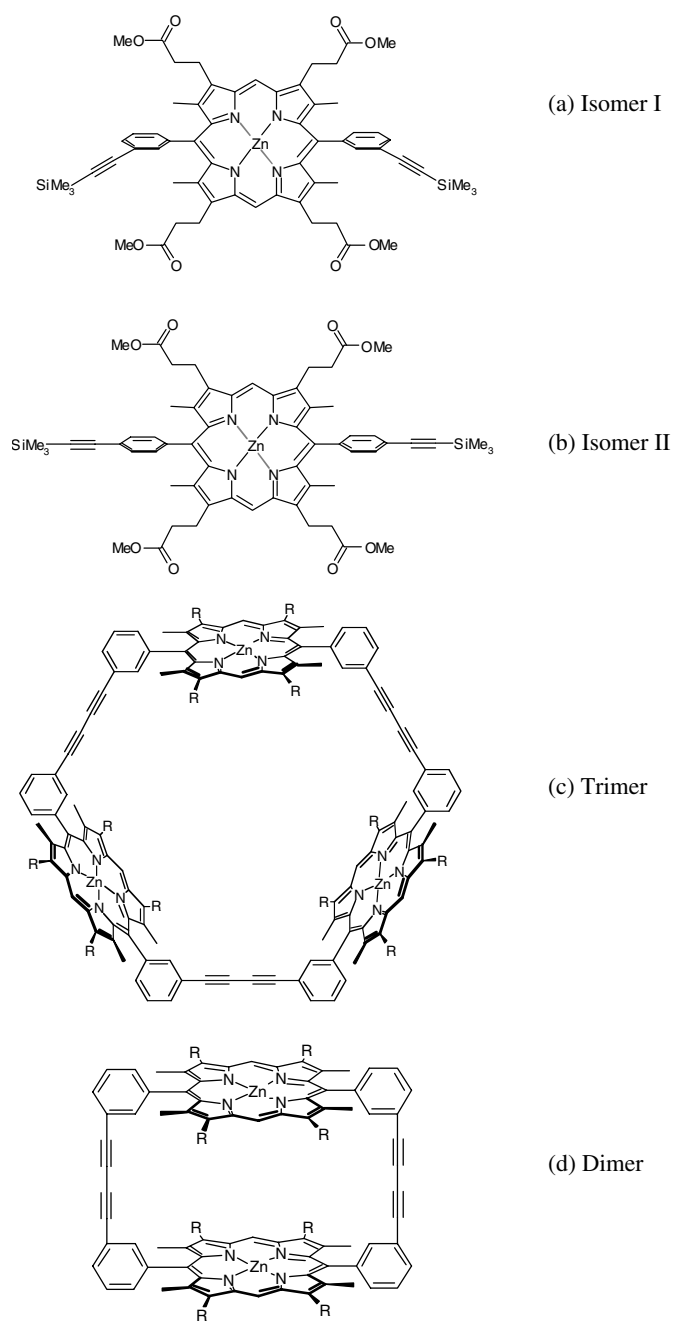


Figure 1. Schematic molecular structures of the four porphyrin molecules used in the experiments. (a) Isomer I; (b) isomer II; (c) ZPD; (d) ZPT.

molecule. It is very difficult to obtain single crystals of this trimer molecule suitable for x-ray diffraction analysis. However, x-ray crystallography of related diarylporphyrin monomers [24] indicates that the phenyl plane is nearly perpendicular to the planes of the porphyrin rings, while molecular modelling (CS Chem3D, CambridgeSoft, Cambridge, MA) shows that the

outer diameter of the trimer cavity is 2.7 nm and the height of the trimer should be 1.8 nm. Finally figure 1(d) shows a cyclic zinc porphyrin dimer (ZPD) molecule formed via the same bonding scheme as for the trimer molecule, but with one monomer unit less.

2.2. The deposition procedure

The various zinc porphyrin molecules were each deposited on the surface of freshly cleaved graphite (highly oriented pyrolytic graphite, HOPG). The molecules were first dissolved into a suitable organic solvent and then a droplet of the solution ($\sim 2 \mu\text{l}$) was applied onto the surface, and left to dry in air. During the evaporation of the solvent, the porphyrin molecules self-organize into 2D or 3D structures depending on the initial concentration of the solution as well as the solvent used. The concentration and the volume of the solution were carefully chosen such that the number of porphyrin molecules deposited on the graphite surface was just about enough to form a single molecular layer. Tapping mode AFM imaging of the molecular thin films was performed in air at room temperature with a Dimension 3100 SPM (Digital Instruments, Santa Barbara, CA). STM images were obtained in air using the same Dimension 3100 system with mechanically cut Pt/Ir tips.

3. Results and discussion

3.1. Influence of the molecular structure on the molecular film

The addition of various side chains onto the porphyrin main frame to modify, e.g., the solubility in a particular solvent is also expected to influence the morphology of the molecular film by modifying the intermolecular interactions. In this section, the molecular structure effect is examined by comparing the structures of the molecular films of the four molecules shown in figure 1. Graphite is the common substrate and the solvent is tetrahydrofuran (THF) in all cases. Figure 2(a) shows an AFM image of the molecular film of isomer **I** on graphite. The rounded dark areas in the image are bare graphite substrate whilst the lighter areas are those covered by the porphyrin molecules. The dark patches resemble the drying spots of a de-wetting liquid film on a solid substrate [25] and are believed to form before the solvent completely evaporates. The faint line running from the top left to the bottom right in the image is due to a step on the graphite substrate. It is notable that the structure of the molecular layer is hardly affected by this step, possibly due to a step height limited in comparison with the size of the molecules. A magnified view of the molecular film of isomer **I** (figure 2(b)) reveals a significant number of grainy dark spots around 10 nm in size, demonstrating clearly the porous nature of this molecular film. Figure 2(c) shows a height profile along the line AB in figure 2(b). According to this line profile, the height of the film is 0.6 nm. The measured height suggests that the graphite surface is covered by no more than one layer of porphyrin molecules. This molecular film will be referred to as the isomer **I** monolayer, despite the voids within the film.

The morphology of the isomer **II** film on graphite is completely different, as shown in figure 3(a). The molecular film in this case consists of separate islands of monolayer height. The definition of a monolayer in this case is based on the fact that all the islands have the same height, which is also the minimum height observed for this isomer. Within each island, the isomer molecules seem to be more densely packed than in the case of isomer **I**, as the number of nanometre sized voids in figure 3(b) is much smaller. The height profile shown in figure 3(c) gives the height of the isomer **II** monolayer to be 1.2 nm, which is much higher than the isomer **I** monolayer (0.6 nm).

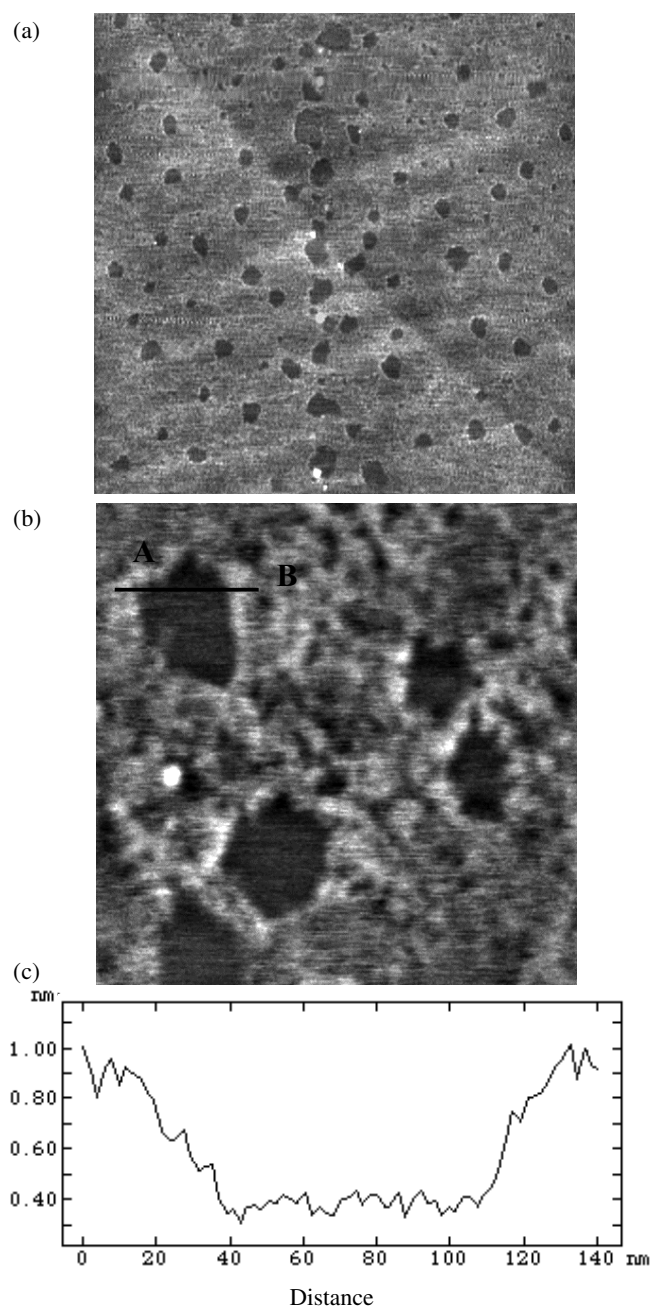


Figure 2. Tapping mode AFM images of a molecular film of isomer I on graphite. (a) $2\ \mu\text{m} \times 2\ \mu\text{m}$; (b) $500\ \text{nm} \times 500\ \text{nm}$; (c) the height profile along line AB in (b).

Because THF was used as the solvent for both isomers and the molecules were adsorbed onto the same graphite substrate, it is reasonable to conclude that the different morphologies of the molecular monolayers of the two isomers are due to the difference in their molecular structures. As discussed earlier, the structural difference lies in the different positions of the

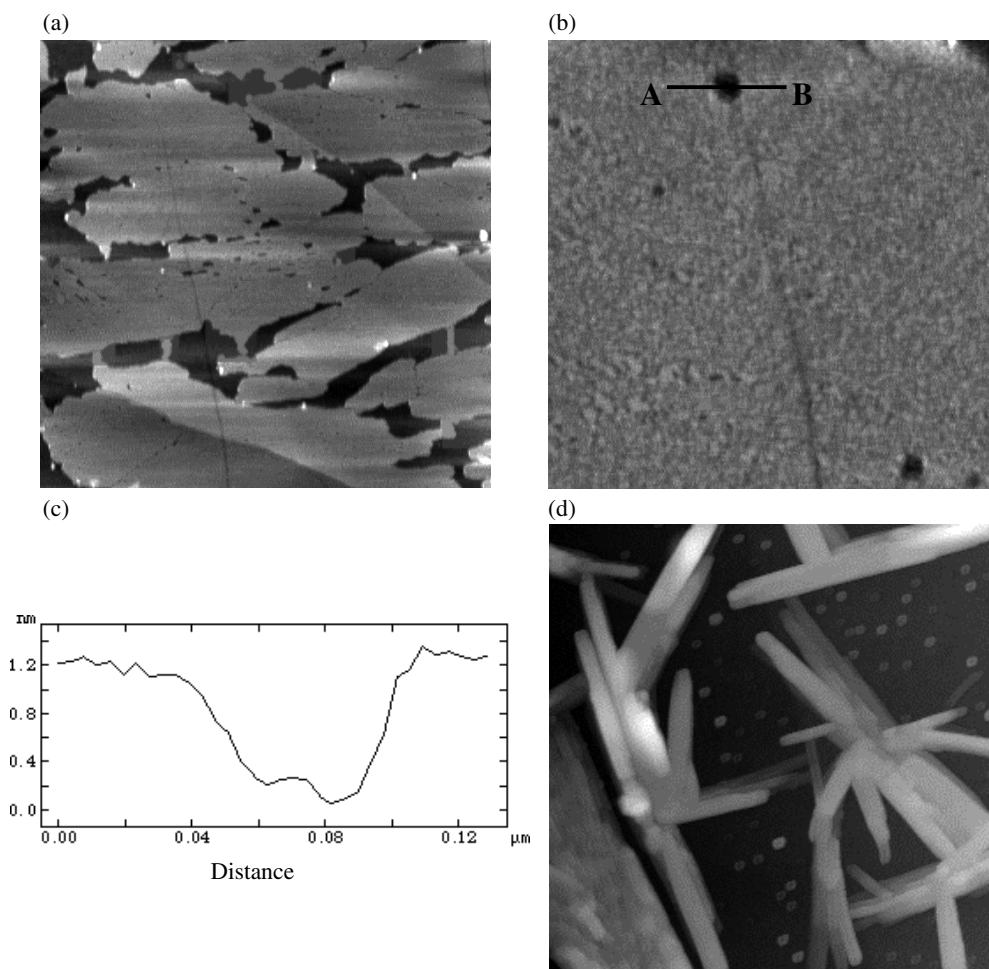


Figure 3. Tapping mode AFM images of a molecular film of isomer II on graphite. (a) $5\ \mu\text{m} \times 5\ \mu\text{m}$; (b) $1\ \mu\text{m} \times 1\ \mu\text{m}$; (c) the height profile along line AB in (b); (d) an AFM image ($5\ \mu\text{m} \times 5\ \mu\text{m}$) of isomer II crystals precipitated from a solution of $3.5 \times 10^{-4}\ \text{M}$. The porphyrin ‘needles’ seen in the figure are about 200 nm in width and 10–20 nm in height.

acetylene linkers on the two isomers. For isomer I, the solvent–substrate interaction seems to dominate the process of film growth, leading to a film morphology similar to that formed by spinodal de-wetting [26]. This suggests that both the molecule–substrate and intermolecular interactions are weak, giving rise to the formation of a loosely packed amorphous film. In contrast, the monolayer islands formed from isomer II are typical of a two-dimensional nucleation and growth process, as observed in many similar systems [27], and suggest a more attractive intermolecular interaction than in the case of isomer I. Each island in figure 3(a) may originate from a single nucleation site. We propose that once an island grows to above a critical size, the attractive force between the island and the graphite substrate becomes strong enough that the island is immobilized and grows by capturing more molecules at the periphery of the island. However, with liquid phase deposition there is always the effect of the solvent film, which confines and carries the solute molecules. The narrow bridges between the islands

(figure 3(a)), which seldom appear in vapour deposited films, are clearly associated with the solvent effect.

The orientation of the molecules within the molecular film cannot be obtained directly from the AFM images. However, from the measured heights of the molecular films, it can be deduced that isomer **II** stands on the surface with two of the four ester chains as two 'legs', while the other two ester chains point away from the surface and the porphyrin ring is approximately perpendicular to the surface. Adjacent molecules are then probably bonded through the usual co-facial stacking of the macrocycles, following the scheme which applies in the bulk of this type of molecular solid. X-ray diffraction data on porphyrin **II** single crystals show that the molecules are stacked off-centre, with three of the ester side arms adopting extended conformations and the fourth side arm curled away to avoid too close contact with the second porphyrin molecule [28]. We note that when higher concentration solutions of isomer **II** were used, large needle-like porphyrin crystals were observed to form on the surface, indicating preferential growth in the direction perpendicular to the macrocycle rings (figure 3(d)).

Crystallization of isomer **I** through the same co-facial packing process is rather unfavourable. This is due to the positions of the TMS groups, which are *meta*-substituted (figure 1(a)). As a result, the two TMS groups in isomer **I** can take two energetically equivalent configurations: a *cis* form, in which the two TMS groups stick out on the same side of the macrocycle, and a *trans* form, in which the two TMS groups lie at opposite sides of the plane (the schematic diagram shown as figure 1(a) shows the *cis* form). Statistically 50% of the molecules adopt the *cis* form and the rest adopt the *trans* form. Because of the two possible configurations, crystallization of isomer **I** via co-facial stacking becomes very much restricted due to steric hindrance. This explains why large aggregates of isomer **I** would not form within the THF solvent and all the molecules remain fairly scattered over the surface until the final stage of evaporation, when they are dragged together into a loose assembly by capillary forces. The much lower height (0.6 nm) of the isomer **I** molecular film suggests that the molecules are probably sitting on the surface with the plane of the macrocycle approximately parallel to the substrate. Then the measured height of the molecular film may arise from the TMS groups which point away from the surface.

The structure of the ZPT film on graphite has been reported previously [22, 29]. A typical AFM image of the trimer film is shown as a reference in figure 4(a) (from [20]). The structure of a typical ZPD monolayer on graphite is shown in figure 4(b). Despite some similarity between the molecular structure of the dimer and the trimer and the fact that the same solvent and substrate were used, the molecular films appear distinctly different. In the case of the trimer, the molecular film does not show any long range order. This is due to the intrinsic difficulty in crystallization of the trimer molecules, as evidenced by figure 4(c). The micrometre sized structures shown in figure 4(c) were formed on graphite with a trimer solution of higher concentration (1.4×10^{-4} M). In this case, once the evaporation of the THF solvent occurred, the concentration quickly increased to a level where precipitation took place. The irregular shape of the trimer aggregates shown in figure 4(c) points to the absence of any preferred growth direction, in contrast to the regular columnar crystals of isomer **II** (figure 3(d)).

The orientation of the trimer molecules within the molecular monolayer has been identified previously [22]. It was shown that the trimer molecule stands on the surface with six ester chain 'legs', such that the plane of each of the three macrocycles is approximately perpendicular to the surface. The dimer film, however, consists of two contrasting phases: one phase with a net-like structure and the other in the form of densely packed islands. The height of the dimer islands shown in figure 4(b) as measured with the AFM is the same as the height of the trimer monolayer, i.e. 1.5 nm. Thus, the dimer molecules are believed to adopt the same adsorption

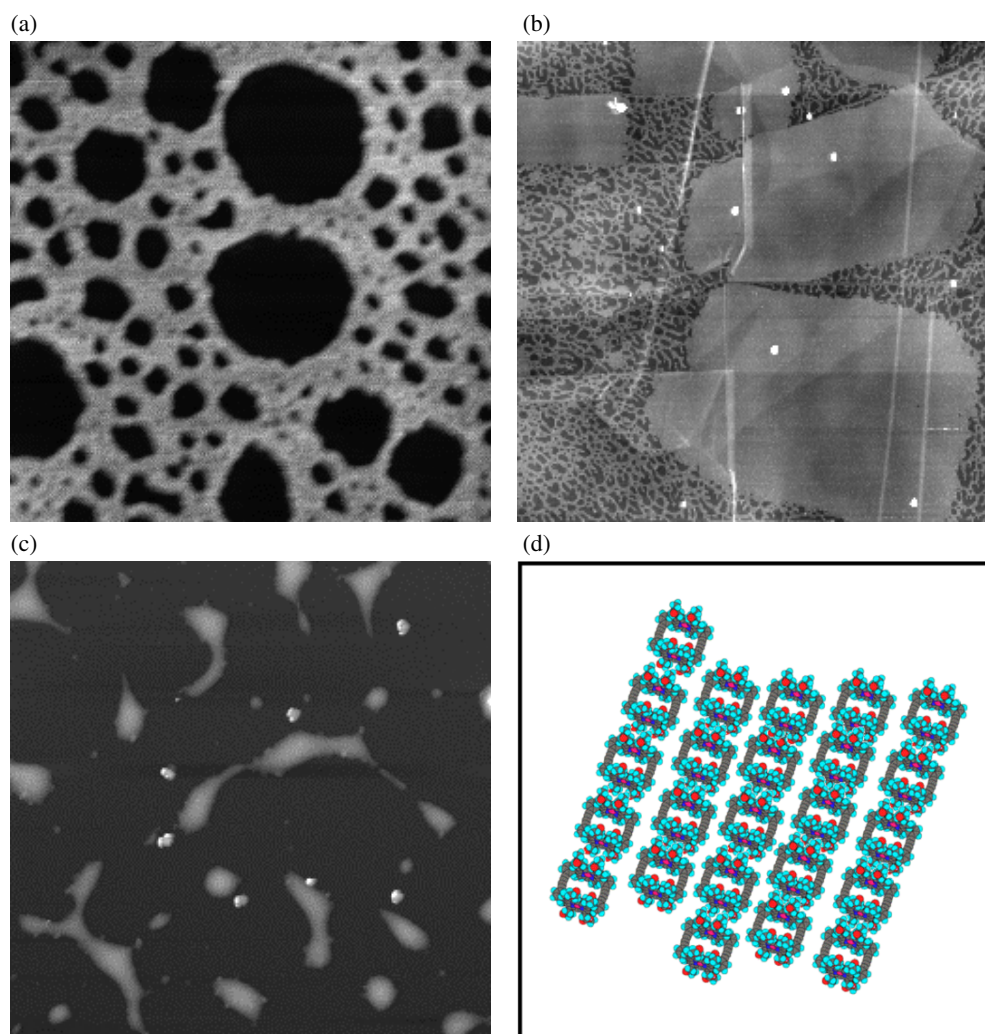


Figure 4. (a) A tapping mode AFM image ($1\ \mu\text{m} \times 1\ \mu\text{m}$) of a ZPT film on graphite (from [20]); (b) a tapping mode AFM image ($10\ \mu\text{m} \times 10\ \mu\text{m}$) of a ZPD film on graphite; (c) a tapping mode AFM image ($10\ \mu\text{m} \times 10\ \mu\text{m}$) showing the precipitated ZPT solids; (d) a schematic diagram of the proposed structure of the ZPD monolayer.

(This figure is in colour only in the electronic version)

orientation as the trimer molecules (macrocycles perpendicular to the surface), the only way for the dimer and trimer monolayers to have the same height.

The dense islands of the dimer molecules are found to show some regular shapes. For instance, the island near the top left hand corner of figure 4(b) has a clear rectangular shape. This suggests that the islands grow preferentially along certain directions and are probably in the form of two dimensional crystals. Figure 4(d) shows a proposed structural model for an ordered dimer film. The scheme shown in this figure allows the co-facial packing of the macrocycles, as preferred by this class of molecules. The fast growth direction is then perpendicular to the plane of the macrocycles. It is possible that these molecules can accommodate a certain

level of strain, introduced as a result of the intermolecular bonding. In the case of the trimer molecules, it seems that the strain involved is probably too high to allow proper molecular bonding to take place, leading to the formation of an amorphous layer.

The two phases present in the dimer monolayer are probably formed at different stages in the solvent evaporation process. The dense islands are probably nucleated at surface defect sites, and grow by capturing molecules at the island boundaries, i.e., those molecules within the molecular diffusion length. Given enough time, all molecules should become attached to the islands in this manner. However, the liquid solvent film is evaporating and ruptures at some critical thickness, carrying the remaining molecules laterally into a foam-like structure which leads to the formation of the net-like phase.

3.2. The effect of the solvent

In this section, the morphology of the ZPT and dimer films prepared using THF is compared with that obtained using toluene. The solubility of the trimer molecule in THF is good, and it is easy to prepare solutions with concentrations from 10^{-7} to 10^{-3} M. Moreover, THF completely wets the graphite surface and is thus able to distribute the porphyrin molecules evenly across the substrate. When a 1–2 μl droplet of 3×10^{-5} M trimer solution is applied to the surface, it gives rise to a molecular coverage close to a complete monolayer. The solubility of ZPT in toluene, on the other hand, is much lower, with a saturation concentration below $\sim 10^{-6}$ M. This low solubility, coupled with the poorer wetting of graphite by toluene, prevents the formation of extended porphyrin monolayers when toluene is evaporated. Figure 5(a) shows an AFM image of ZPT film on graphite prepared using toluene. Rounded islands, in this case 1.5 nm in height and mostly separated from one another, are seen in the image. Step edges and line defects on graphite seem to play a much more important role. For example, a ‘line’ of ZPT molecules can be seen running diagonally near the top right corner of the image, formed along a line defect on graphite.

Figure 5(b) shows an AFM image of ZPD molecules on graphite also prepared using toluene. Molecular islands one monolayer in height, similar to those in figure 5(a), are observed. Once again a number of these islands are associated with a common defect line on graphite. Arrows are drawn into figure 5(b) to assist the eye to identify the two defect lines. The density of the molecular islands as a whole is of the order of 4×10^8 to $1 \times 10^9 \text{ cm}^{-2}$, which is remarkably close to the density of naturally existing defects on a typical cleaved graphite surface [30, 31]. Therefore, it is quite likely that all islands are associated with surface defects. It is notable that when THF is used as the solvent, surface defects and step edges do not seem to play any role at all in the formation of the ZPT molecular layers. This suggests that toluene has a stronger affinity towards surface defects and that the images shown in figure 5 can be explained as follows. The initially continuous toluene film breaks up at some critical thickness by disintegrating into a large number of small micro-droplets; each droplet is located around a surface defect. Sometimes two neighbouring droplets may interconnect, leading to the formation of elongated islands such as those shown in figure 5(a). As a droplet shrinks due to evaporation, the molecules within each droplet are carried towards the location of the defect where a molecular island is formed. The average island size is dependent on the number of porphyrin molecules inside each droplet and is thus determined by the initial concentration of the solution. In the case of toluene, the concentration is limited by the solubility of the molecules and even with a saturated solution the final molecular coverage on graphite is always lower than 0.1 ML.

The solubility of porphyrin molecules in toluene can be improved significantly by adding a small amount ($\sim 10^{-5}$ M) of DABCO (1,4-diazabicyclo-octane). DABCO is a bidentate

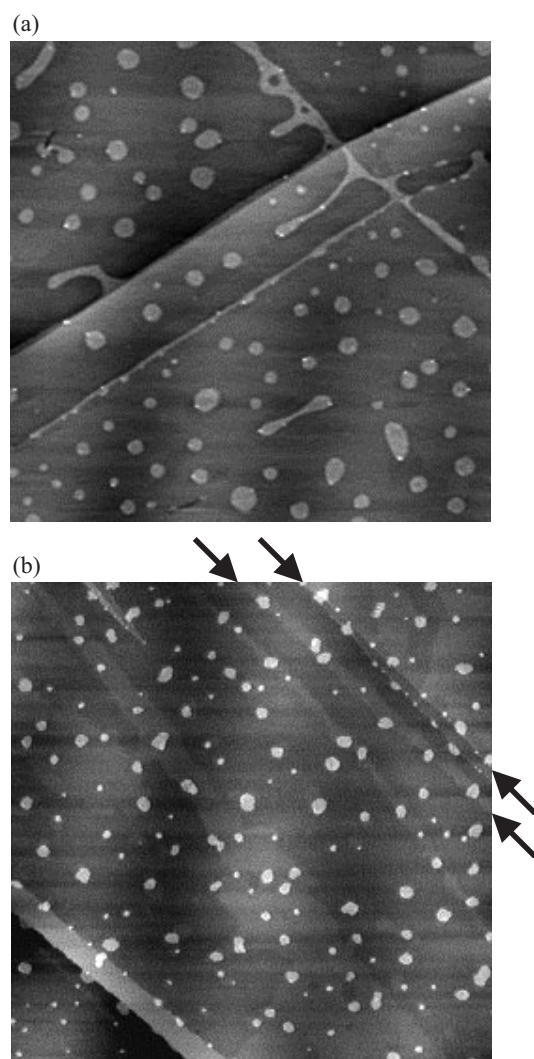


Figure 5. Tapping mode AFM images of ZPT and ZPD islands on graphite deposited with solutions of toluene. (a) One monolayer high ZPT islands on graphite ($5\ \mu\text{m} \times 5\ \mu\text{m}$); (b) one monolayer high ZPD islands on graphite ($5\ \mu\text{m} \times 5\ \mu\text{m}$).

ligand and functions as a bridge between the metal cations in the centres of the two porphyrin rings [32]. When DABCO is added to ZPT with a 1:1 molecular ratio and dissolved in toluene, it is possible to produce a molecular coverage on graphite well above 0.1 ML. Figure 6 shows an AFM image of a trimer film prepared in toluene solution with added DABCO. The structure of the molecular film shown in figure 6 is distinctly different from that shown in figure 5(a). Instead of separate islands, a continuous, two-dimensional molecular network one monolayer in height is formed. Since there is no extended dense porphyrin island and the overall appearance of the network resembles a foam, it is clear that the addition of DABCO is not sufficient to crystallize the trimer molecules. However, DABCO does play an important role in the structuring of the molecular film. The DABCO molecules must remain on the surface after the evaporation of toluene, either as a separate phase of DABCO crystals or by incorporation into the trimer

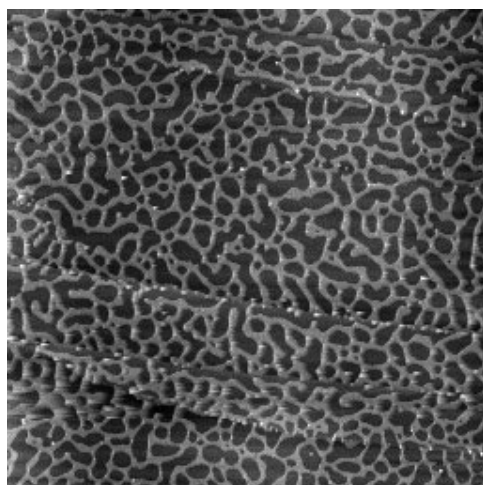


Figure 6. An AFM image ($10\ \mu\text{m} \times 10\ \mu\text{m}$) of a ZPT film on graphite, prepared using toluene with added DABCO.

aggregates. There is no evidence of phase separation in the AFM images, so it seems that the DABCO molecules are mixed with the trimer molecules, thus influencing the formation of the two dimensional networks.

4. Conclusions

The influence of the molecular structure, the solvent and the substrate on the formation of monolayers of supramolecular films has been investigated, using zinc porphyrins as a testing example. It has been shown that a range of interesting molecular structures can be deposited onto a solid substrate from liquid sources. By controlling the concentration of the starting solution and the amount of liquid applied to the graphite surface, single layer high molecular weight films can be successfully grown with a variety of zinc porphyrin molecules. The nucleation and growth, similar to those commonly observed in vapour deposition, have been found to depend on the strength of the intermolecular interaction as well as the level of interaction between the solvent molecules and the substrate.

Acknowledgments

This work was supported by the Leverhulme Trust and the EPSRC.

References

- [1] Carter F L, Siatowski R E and Wholtjen H (ed) 1988 *Molecular Electronic Devices* (Amsterdam: North-Holland)
- [2] Aviram A (ed) 1989 *Molecular Electronics: Science and Technology* (New York: Engineering Foundation)
- [3] Drury C 1998 *Appl. Phys. Lett.* **73** 108
- [4] Garnier F, Hajlaoui R, Yassar A and Srivastava P 1994 *Science* **265** 1684
- [5] Kido J, Kimura M and Nagai K 1995 *Science* **267** 1332
- [6] Burroughes J H, Bradley D D C, Brown A R, Marks R N, Mackay K, Friend R H, Burn P L, Kraft A and Holmes A B 1990 *Nature* **347** 530
- [7] Greenham N C, Moratti S C, Bradley D D C, Friend R H and Holmes A B 1993 *Nature* **365** 628
- [8] Braun D and Heeger A J 1991 *Appl. Phys. Lett.* **58** 1982

- [9] Balzani V and Scandola F 1996 *Comprehensive Supramolecular Chemistry* vol 10, ed J L Atwood, J E D Davies, D D MacNicol and F Vogtle (Oxford: Pergamon) p 687
- [10] Hunter C A and Sanders J K M 1990 *J. Am. Chem. Soc.* **112** 5525
- [11] Malinski T and Taha Z 1992 *Nature* **358** 676
- [12] Davila J, Harriman A and Milgrom L R 1987 *Chem. Phys. Lett.* **136** 427
- [13] Gimzewski J K and Joachim C 1999 *Science* **283** 1683
- [14] Jung T A, Schlitter R R, Gimzewski J K, Tang H and Joachim C 1996 *Science* **271** 181
- [15] Yokoyama T, Yokoyama S, Kamikado T, Okuno Y and Mashiko S 2001 *Nature* **413** 619
- [16] Umbach E, Glockler K and Sokolowski M 1998 *Surf. Sci.* **402–404** 20
- [17] Sleator T and Tycko R 1988 *Phys. Rev. Lett.* **60** 1418
- [18] Upward M D, Beton P H and Moriarty P 1999 *Surf. Sci.* **441** 21
- [19] Rosei F, Schunack M, Naitoh Y, Jiang P, Gourdon A, Laegsgaard E, Stensgaard I, Joachim C and Besenbacher F 2003 *Prog. Surf. Sci.* **71** 95
- [20] Moresco F, Meyer G, Rieder K H, Tang H, Gourdon A and Joachim C 2001 *Appl. Phys. Lett.* **78** 306
Moresco F, Meyer G, Rieder K H, Tang H, Gourdon A and Joachim C 2001 *Phys. Rev. Lett.* **86** 672
- [21] Schreiber F 2000 *Prog. Surf. Sci.* **65** 151
- [22] Yin J, Guo Q, Palmer R E, Bampos N and Sanders J K M 2003 *J. Phys. Chem. B* **107** 209
- [23] Bampos N, Marvaud V and Sanders J K M 1998 *Chem. Eur. J.* **4** 335
- [24] Bond A D, Feeder N, Redman J E, Teet S T and Sanders J K M 2002 *Cryst. Growth Dev.* **2** 29
- [25] Thiel U, Mertig M and Pompe W 1998 *Phys. Rev. Lett.* **80** 2869
- [26] Brochard F and Daillant J 1990 *Can. J. Phys.* **68** 1084
- [27] Brune H 1998 *Surf. Sci. Rep.* **31** 121
- [28] Bampos N, Princep M R, He H, Vidal-Ferran A, Bashall A, McPartlin M, Powell H and Sanders J K M 1998 *J. Chem. Soc. Perkin Trans.* **2** 715
- [29] Palmer R E and Guo Q 2002 *Phys. Chem. Chem. Phys.* **4** 4275
- [30] Darby T P and Wayman C M 1975 *J. Cryst. Growth* **28** 41
- [31] Anton R and Schneiderei I 1998 *Phys. Rev. B* **58** 13874
- [32] Hunter C A and Tregonning R 2002 *Tetrahedron* **58** 691